

Pulse-Technique Analysis of the Kinetics of the Fischer-Tropsch Reaction

F. M. DAUTZENBERG, J. N. HELLE, R. A. VAN SANTEN, AND H. VERBEEK

Koninklijke/Shell-Laboratorium, Amsterdam, Shell Research B.V., The Netherlands

Received November 25, 1976; revised May 18, 1977

In the Fischer-Tropsch synthesis of paraffins the use of transient operating conditions can influence the molecular weight distribution of the product in that these conditions enable the formation of high molecular weight compounds to be inhibited. The molecular weight distributions obtained can be described by a simple kinetic model which, when applied to the experimental results, provides numerical data on the rate constants of the propagation reaction. With two differently prepared Ru/ γ -Al₂O₃ catalysts it has been found that, under transient operating conditions, the chains grow at a rate of about one CH₂ group per minute. The low overall activity of these catalysts appears to be due to the very low intrinsic activity of the exposed Ru atoms and not to a low number of active surface atoms.

INTRODUCTION

The scarcity of liquid fossil fuels and the relative abundance of coal have refocused attention on the possibility of producing hydrocarbons via the Fischer-Tropsch synthesis. In this reaction, depending on the choice of catalyst and the operating conditions, carbon monoxide is catalytically hydrogenated to give mainly paraffins, olefins, and/or oxygen-containing compounds. The reaction product usually contains a wide range of hydrocarbons of different chain lengths, due to the fact that the Fischer-Tropsch synthesis can be described (1) as being essentially a polymerization process comprising initiation, propagation, and termination steps. On the basis of modern developments in carbonyl chemistry, it is now generally accepted that carbon monoxide and hydrogen react in the adsorbed state to form a primary oxygen-containing chemisorption complex (initiation). This step is followed by chain growth via successive insertion of carbon

monoxide, hydrogenation of the resulting intermediate, insertion of carbon monoxide, etc. (propagation) (2). Finally, the last step consists in desorption of the hydrogenated product (termination).

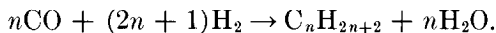
All the catalysts known for this process, however, show an activity that is several orders of magnitude lower than that usually found in heterogeneous catalysis. In a series of articles on the methanation of carbon monoxide by hydrogen, Vannice (3) has convincingly shown that the catalytic activity per unit surface area of exposed metal, the specific activity, is very small indeed. Since the activation energies are not unusually high, one finds very low pre-exponential factors. The question then remains whether this is due to the fact that only very few exposed surface atoms are active or that the surface atoms themselves have a very low intrinsic activity. Unlike the rate of initiation, which is proportional to the number of active surface atoms, the rates of propagation and termination should be independent of the number

of active centers, since it is commonly assumed that chain growth takes place via insertion (3), as mentioned above.

The primary aim of our study, therefore, was to determine the rate of propagation so as to obtain a measure of the intrinsic activity of the catalyst atoms. Determination of this rate should in principle be possible by departure from the steady state (4), since in a chain-growth mechanism the rate of relaxation to the steady state is determined by the rate of propagation. Therefore, we used transient operating conditions instead of continuous flow and studied the changes in product distribution.

EXPERIMENTAL

For the sake of simplicity we performed all the experiments with *in situ*-reduced Ru catalysts, because with these catalysts predominantly unbranched polymethylene chains are formed (no CO₂):



For each test a fresh catalyst sample of 3% Ru by wt on $\gamma\text{-Al}_2\text{O}_3$ was taken. Two different preparations were tested, one (catalyst A) prepared by impregnation of a wide-pore $\gamma\text{-Al}_2\text{O}_3$ with RuCl_3 , the other (catalyst B), by deposition of a trimetal atom-cluster carbonyl complex $\text{Ru}_3(\text{CO})_{12}$ on the same type of alumina. The exposed Ru surface areas were determined by O₂ chemisorption measurements.

The reaction conditions were periodically changed as follows: After reduction in hydrogen (16 h, 350°C), a CO/H₂ mixture (1/1) was admitted to a stainless steel microflow reactor containing 25 ml of catalyst at a pressure of 10 bar and a temperature of 210°C over a variable time τ (e.g., $\tau = 4$ min or $\tau = 12$ min). These reaction conditions were selected because they favor a high chain-growth probability. By opening a magnetic valve the CO/H₂ reaction mixture was subsequently replaced by pure hydrogen, while the temperature was raised to 350°C. This was done to enforce

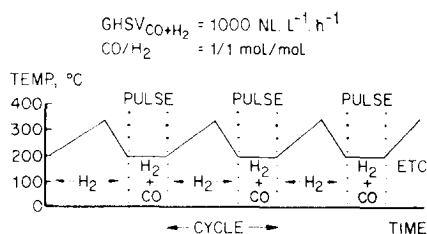


Fig. 1. Schematic presentation of the transient operating conditions used.

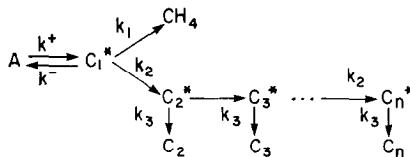
chain termination and product desorption. Next, the catalyst bed was rapidly cooled down from 350 to 210°C. The amount of hydrocarbons obtained in one pulse being insufficient for an analysis, we accumulated the product from a large number of cycles. The procedure applied is schematically indicated in Fig. 1.

At the start of each experiment the outlet of the reactor was directly coupled to a mass spectrometer, which allowed us to follow instantaneously the formation of light hydrocarbons. The dimensions of the reactor used, the gas velocity, and the particle size of the catalyst (50–100 mesh) ensured ideal plug flow during our experiments.

The molar concentrations of the individual paraffinic compounds in the liquid product were determined by temperature-programmed glc analyses. We further measured the amount of water formed during the reaction.

THEORETICAL ANALYSIS

The hydrocarbons are supposed to be formed according to the following scheme.



In this scheme, A represents a precursor generated upon reaction of adsorbed hydrogen and carbon monoxide. C₁*, C₂*, ..., C_n* are the adsorbed intermediates for the formation of hydrocarbons having 1, 2, ...,

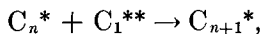
n carbon atoms in the chain. The rate constant of the initiation reaction is given by k^+ ; k_2 is the rate constant of the propagation reaction, and k_1 and k_3 are the rate

constants of the termination reactions of C_1^* and C_2^* , ..., C_n^* , respectively. The kinetic equations to be solved according to this scheme are:

$$\dot{C}_1 = \frac{d[C_1]}{dt} = k_1[C_1^*]; \quad \frac{d[C_1^*]}{dt} = k^+[A] - (k^- + k_1 + k_2)[C_1^*] \quad (1a)$$

$$\left. \begin{aligned} \dot{C}_2 &= \frac{d[C_2]}{dt} = k_3[C_2^*]; & \frac{d[C_2^*]}{dt} &= k_2[C_1^*] - (k_2 + k_3)[C_2^*] \\ \dot{C}_n &= \frac{d[C_n]}{dt} = k_3[C_n^*]; & \frac{d[C_n^*]}{dt} &= k_2[C_{n-1}^*] - (k_2 + k_3)[C_n^*] \end{aligned} \right\} \quad (1b)$$

The essential assumption underlying the kinetic description of the proposed reaction scheme is the time independence of the (pseudo) rate constants k_2 and k_3 . According to the proposed reaction scheme, chain growth takes place, as generally accepted, via conversion of C_n^* into C_{n+1}^* , obviously through addition of a one-carbon-atom-containing species. Since it is not necessary to rule out the possibility of one-carbon-atom-containing species other than C_1^* or CO being present at the catalyst surface, we will denote the unit to be inserted by the symbol C_1^{**} . It will be clear that, for the kinetic treatment of the chain growth reaction,



the chemical nature of C_1^{**} is irrelevant. Regardless of whether or not C_1^{**} contains oxygen, for instance, the rate of propagation is given by:

$$R_{\text{prop}} = k_2' \cdot [C_1^{**}] \cdot [C_n^*].$$

It seems reasonable to assume that C_1^{**} is in a less hydrogenated state than is C_1^* . As will be discussed below, our results are consistent with C_1^* being at steady state, which allows us to assume that this is also the case for C_1^{**} . Therefore, we have used

$$k_2 = k_2' \cdot [C_1^{**}]$$

as the rate constant of propagation in our kinetic scheme.

The termination reaction can be represented as



The rate of termination is then given as:

$$R_{\text{term}} = k_3' \cdot (p_{H_2})^x \cdot [C_n^*].$$

Since we operated at low conversion levels the partial pressure of H_2 (and also that of CO) is virtually independent of time. Consequently,

$$k_3 = k_3' \cdot (p_{H_2})^x$$

may be used in the above kinetic scheme.

At steady state the set of equations (1b) can easily be solved. From this, the molar concentrations of the compounds in the product are found to be proportional to α^{n-1} . The probability of chain growth α is a constant defined by:

$$\alpha = \frac{\dot{C}_n}{\dot{C}_{n-1}} = \frac{k_2}{k_2 + k_3}. \quad (2)$$

As shown by Anderson *et al.* (5) this is a good approximation because it enables the experimental product distributions to be described reasonably well, at least for $n > 3$. For a specific catalyst, α can be influenced by changing the temperature, pressure, etc., but for steady-state operation this only results in a shift of the product distribution. If the molar concen-

trations of the compounds are plotted on a logarithmic scale versus chain length the result is a straight line with slope $\log \alpha$.

In our experiments, however, we intentionally used transient operating conditions. It will be shown below that, beyond a certain chain length, the formation of high molecular weight products will decrease steeply under such conditions, because according to our reaction scheme only those species will grow that remain adsorbed at the catalytic surface throughout the pulse. The applied pulse time τ , therefore, is the critical parameter by which the product distribution can be influenced.

The amount of hydrocarbons of chain length n produced after one CO/H₂ pulse of time τ is:

$$P_n(\tau) = \int_0^\tau dt' [\dot{C}_n(t')] + \alpha [C_n^*(\tau)]. \quad (3)$$

This is the sum of the amount of hydrocarbons formed during the pulse and the amount of hydrocarbons desorbed from the surface during the temperature-program period in pure hydrogen.

The general solutions of Eqs. (1) at time t after the start of the CO/H₂ pulse are:

$$\begin{aligned} [C_n^*(t)] &= e^{-(k_2+k_3)t} k_2^{n-1} \int_0^t dt_{n-1} \int_0^{t_{n-1}} dt_{n-2} \\ &\quad \dots \int_0^{t_2} dt_1 e^{(k_2+k_3)t_1} [C_1^*(t_1)] \\ &\quad (n \geq 2) \end{aligned} \quad (4a)$$

$$\begin{aligned} [C_1^*(t)] &= k + \int_0^t dt' e^{-(k_1+k_2+k^-)(t-t')} [A(t')]. \end{aligned} \quad (4b)$$

The behavior of $\dot{C}_n(t)$ as a function of t can now be calculated if the time evolution of $A(t)$ is known. With respect to the behavior of $[A(t)]$ two extreme postulates can be made.

(i) The intermediate A is only formed at the start of the CO/H₂ pulse, covering all available sites ($\theta \approx 1$). During the pulse, A is converted into C₁^{*}, etc., but no additional A is formed which can be converted into hydrocarbon products. The expression for $[A(t)]$ then becomes:

$$[A(t)] = e^{-k^+ \cdot t} [A(0)]. \quad (5)$$

(ii) The concentration of A is independent of time and can also be formed during the CO/H₂ pulse. This postulate is consistent with the rate of conversion of A being small compared with its rate of formation and simply implies that A is at steady state. In this case:

$$[A(t)] = \text{constant}. \quad (6)$$

In order to illustrate the basic difference between postulates (i) and (ii) we calculated the relative molecular product distributions for two pulse times. To this end we solved the equations for both cases, assuming for simplicity that $k_3 = k^- = 0$ and adopting an equal value for all other rate constants. The results for these two situations are plotted in Fig. 2. Whereas in case (i) a narrow distribution around a mean value is found, a very different product distribution is observed in case (ii). In both cases the production of long-chain hydrocarbons can be controlled by varying the pulse length. The second model, however, predicts that the front-end product distribution approaches the steady-state

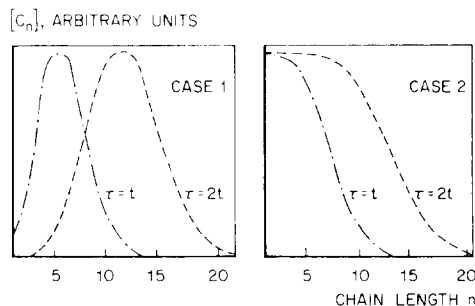


FIG. 2. Relative molecular product distributions for two pulse times.

distribution. This can be understood if one realizes that initiation of the reaction continues during the pulse. Thus, the pattern in case (ii) can be considered to be a superposition of curves similar to those in case (i) but displaced to shorter times.

Our experimental data (see Fig. 3) appear to be in agreement with the second model. For this situation, Eqs. (4) can be readily evaluated, if we further assume that $C_1^*(t)$ is at steady state:

$$C_1^*(t) = C_1^*(\infty) = \frac{k^+}{k_1 + k_2 + k^-} [A]. \quad (6)$$

As will be shown below this is a reasonable assumption since deviations from the steady-state product distribution will only be large for high values of n . Substituting expression (6) into expression (4a) and performing the integrations in (4a) one finds for $[C_n^*(t)]$:

$$\begin{aligned} [C_n^*(t)] &= \alpha^{n-1} \cdot C_1^*(\infty) \cdot f(x, n) \\ &= C_n^*(\infty) \cdot f(x, n), \end{aligned} \quad (7)$$

where $C_n^*(\infty)$ is the steady-state value of C_n^* . The function $f(x, n)$ is given by:

$$f(x, n) = 1 - e^{-x} \left(1 + \sum_{i=1}^{n-2} \frac{1}{i!} x^i \right), \quad (8)$$

whereby $x = (k_2 + k_3)t$.

It will be clear that, for finite times, $f(x, n)$ will be smaller than 1 and will decrease with n . Consequently, we expect that the formation of intermediates leading to high molecular weight products will be suppressed if, instead of steady-state conditions, transient operating conditions are used. In that case the deviations from the steady-state product distribution are expected to become larger with increasing chain length.

Insertion of Eq. (7) into expression (3) gives:

$$\begin{aligned} P_n(\tau) &= \alpha^n \cdot \{ (1 - \alpha) \cdot h[n, x(\tau)] \\ &+ \alpha \cdot f[n, x(\tau)] \} \cdot C_1^*(\infty) \text{ for } (n > 2) \end{aligned} \quad (9)$$

with

$$\begin{aligned} h[n, \alpha(\tau)] &= x + (n-1)(e^{-x} - 1) \\ &+ e^{-x} \cdot \sum_{i=1}^{n-2} (n-i-1) \cdot \frac{x^i}{i!} \text{ for } (n > 2), \end{aligned} \quad (10)$$

where $\alpha \cdot f[n, x(\tau)] \cdot \alpha^n$ represents the amount of product hydrogenated at the end of the pulse, while $(1 - \alpha) \cdot h[n, x(\tau)] \cdot \alpha^n$ gives the amount of product formed during the pulse.

We used expression (9) to fit the experimental results. In this way we determined the values of α and x . Since the pulse time τ is also known, one can calculate k_2 and k_3 .

RESULTS

The amount of water produced is nearly proportional to the H_2/CO -pulse time. As the oxygen from the carbon monoxide is completely converted to oxygen in water, this implies that the formation of hydrocarbons predominantly takes place during the H_2/CO pulse. This enables us to determine the overall rate of CO consumption, k_{overall} . The results are given in Table 1.

Representative relative liquid product concentrations as a function of chain length have been plotted in Fig. 3. This figure shows the product distributions obtained in 8- and 12-min-pulse experiments with catalysts A and B, respectively, together with the best fits of Eq. (9) to the experimental data. In both cases the agreement found is satisfactory.

The rate constants of the propagation and termination reactions derived from Eq. (9) have been listed in Table 1. For catalyst A we also indicated k_{overall} , which represents the turnover number of this catalyst, expressed as moles of CO converted per exposed Ru atom per second. This number could be calculated from the amount of water formed during the reaction and the measured exposed Ru surface area.

TABLE 1
Characteristic Rates for Two Differently Prepared Ru/ γ -Al₂O₃ Catalysts

Catalyst	Pulse time (min)	k_{overall} s ^{-1a}	$k_{\text{propagation}}$ (s ⁻¹)	$k_{\text{termination}}$ (s ⁻¹)	Space time yield (mg · ml ⁻¹ · h ⁻¹)
A	8	1.6×10^{-2}	1.4×10^{-2} 1.6×10^{-2}	7.3×10^{-4} 8.3×10^{-4}	70
B	12	—	1.6×10^{-2}	8.3×10^{-4}	110

^a Assuming all exposed metal atoms to be active.

DISCUSSION AND CONCLUSIONS

The liquid products obtained in our experiments have a very narrow molecular weight distribution. For instance, in the liquid product obtained during the 8-min-pulse experiment, the C₁₂H₂₆/C₆H₁₄ molar ratio is 0.12, whereas a value of 0.74 would have been found if steady-state operation had been applied at the same probability of chain growth ($\alpha = 0.95$). In our experiments the concentrations of the compounds are not proportional to α^{n-1} , and, with increasing chain length n , the deviations from the steady-state distributions become progressively larger, as predicted by our kinetic model.

The distributions of the liquid products in the C₆–C₂₀ range show a striking resemblance to the theoretical curves, justifying the assumption that, during the pulse, the surface concentration of growing precursors remains constant. Increasing the pulse time enhances the production of long-chain hydrocarbons, whereas the distribution of the light hydrocarbons approaches that obtained in steady-state operation.

The good agreement between experiment and theory, therefore, demonstrates that, in principle, application of transient operating conditions permits the determination of the rate constant of the propagation reactions. To our knowledge, this important parameter, characterizing hydrocarbon-synthesis catalysts, has not been determined so far. Although the catalysts

made from the carbonyl complex gave a considerably higher space-time yield than the one prepared by impregnation of Al₂O₃ with RuCl₃, they both gave about the same rate constant, viz., 1.5×10^{-2} s⁻¹. This firmly substantiates our opinion that the method can be used to determine this intrinsic catalyst characteristic. The low rate constant of the propagation reaction corresponds to a growth rate of ca. one –CH₂– group per minute for each growing precursor.

The total amount of hydrocarbon of a particular chain length $P_n(\tau)$ can be determined for the hydrocarbons in the liquid

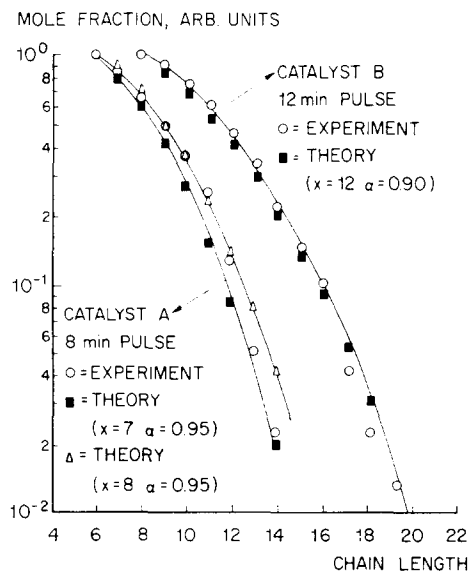


FIG. 3. Liquid product distributions over two Ru/ γ -Al₂O₃ catalysts under transient operating conditions.

fraction of the product. This allows us to calculate the steady-state concentration $C_1^*(\infty)$ from Eq. (9). During the 8-min-pulse experiment with catalyst B, for instance, 0.93×10^{-2} g of $C_{10}H_{22}$ is formed. Using the values of k_2 and k_3 reported in Table 1 we then find $C_1^*(\infty) = 0.026 \times 10^{-2}$ mol. Since we also know the number of exposed Ru atoms as determined by chemisorption (1.2×10^{21} atoms), the surface coverage with $C_1^*(\infty)$ is 0.13. For other chain lengths similar values were found. This value, together with Eq. (7) with $f(x, n) = 1$, enables us to calculate the total steady-state surface coverage with growing chains. We found $\theta_{\text{total}} \approx 0.7$. This means that a large number of the exposed Ru atoms are really active. Thus, the very low activity of these Ru/ γ - Al_2O_3 Fischer-Tropsch catalysts is due not to a low number of active sites, but to the very low intrinsic activity of the Ru atoms.

Recently, the kinetics of hydrocarbons formation and of the methanation reaction over supported Ni and Ru have been reported by Dalla Betta *et al.* (6). The kinetics of the methanation reaction over other supported Group VIII metals as catalysts have been published by Vannice (3). In both cases it was found that the reaction could be fitted to a power rate law of the form:

$$r_{\text{hydrocarbon}} = A[\exp - (E/RT)]p_{H_2}^x \cdot p_{CO}^y,$$

where, for all metals, $x > 0$ and $y \leq 0$. The negative value of y suggests that the rate

of the reaction is limited because the CO molecules are bonded too strongly. This is in agreement with the point of view presented: All the atoms on the surface are active but their reactivity is low.

From the presence of an effect of pulse operation on the product distribution, we conclude that the rate of initiation on heterogeneous Ru catalysts is *not* rate limiting for the Fischer-Tropsch reaction, and that the propagation activity of the atoms catalyzing this reaction is very low.

REFERENCES

1. (a) Storch, H. H., Golumbic, N., and Anderson, R. B., "The Fischer-Tropsch and Related Syntheses," New York: Wiley, 1951; (b) Anderson, R. B., Hofer, L. J., and Storch, H. H., *Chem. Ing. Tech.* **30**, 560 (1958); (c) Pichler, H., Firnhaber, B., Kioussis, D., and Dwallu, A., *Makromol. Chem.* **70**, 12 (1964); (d) Sternberg, H. W., and Wender, J., "International Conference on Coordination Chemistry," p. 54, London, 1959; (e) Roginsky, S. Z., "Proceedings, Third Congress on Catalysis, Amsterdam, 1965," p. 939; (f) Kölbel, H., in "Chemische Technologie" (K. Winnacker and L. Küchler, Eds.), Vol. 3, pp. 439, 452. C. Hauser, München, 1959.
2. Henrici-Olivé, G., and Olivé, S., *Angew. Chem.* **88**, 144 (1976).
3. (a) Vannice, M. A., *J. Catal.* **37**, 449 (1975); (b) Vannice, M. A., *J. Catal.* **37**, 462 (1975); (c) Vannice, M. A., *J. Catal.* **40**, 129 (1975).
4. Boudart, M., "Kinetics of Chemical Processes," p. 79. Englewood Cliffs, N.J.: Prentice-Hall, 1968.
5. Anderson, R. B., Friedel, R. A., and Storch, H. H., *J. Chem. Phys.* **19**, 313 (1951).
6. Dalla Betta, R. A., Piken, A. G., and Shelef, M., *J. Catal.* **35**, 54 (1974).